Fractals, Vol. 11, Supplementary Issue (February 2003) 205–216
© World Scientific Publishing Company

SCALING IN THE ATMOSPHERE: ON GLOBAL LAWS OF PERSISTENCE AND TESTS OF CLIMATE MODELS

ARMIN BUNDE
Institute of Theoretical Physics, Justus-Liebig-University Giessen
Heinrich-Buff-Ring 16, 35392 Giessen, Germany

SHLOMO HAVLIN
Department of Physics, Bar Ilan University, Israel

Abstract

Characterizing the complex atmospheric variability at all pertinent temporal and spatial scales remains one of the most important challenges to scientific research today.[1–5] The main issues are to quantify, within reasonably narrow limits, the potential extent of global warming, and to downscale the global results in order to describe and quantify the regional implications of global change.

1. INTRODUCTION

To face these challenges, atmospheric and oceanographic research usually proceeds along two main paths that we are going to decribe next: (i) Analysis of available meteorological records by appropriate time series analysis techniques, and (ii) generation of and analysis of observation-based, interpolated or model simulated weather and climate records, respectively, through the use of a hierarchy of simulation models.

1.1 Analysis of Meteorological Methods

Among the standard mathematical techniques that have been used are calculations of means, variations and power spectra, decomposition into empirical orthogonal functions and/or

principle components. Very recently, more advanced techniques such as detrended fluctuation analysis and wavelet analysis have been used which are able to systematically separate trends from fluctuations at different time scales.

A considerable amount of effort has been devoted to analyzing temporal correlations that characterize the persistence of weather and climate regimes. The persistence of short term weather states is a well-known phenomenon: there is a strong tendency for subsequent days to remain similar, a warm day is more likely to be followed by a warm day than by a cold day and vice versa. The typical time scale for weather changes is about one week, a time period which corresponds to the average duration of so-called "general weather regimes" or "Grosswetterlagen". This property of persistence is often used as a "minimum skill" forecast for assessing the usefulness of short to medium range numerical weather forecasts. Longer term persistence of synoptic regimes up to time scales of several weeks is often related to circulation patterns associated with blocking.[6] A blocking situation occurs when a very stable high pressure system is established over a particular region and remains in place for several weeks, as opposed to the usual time scale of 3–5 days for synoptic systems. As a result the weather in the region of the high remains fairly persistent throughout the period. Furthermore, transient low pressure systems are deflected around the blocking high so that the region downstream of the high experiences a larger than usual number of storms.

There have been also indications that weather persistence exists over many months or seasons,[7] between successive years, and even over several decades.[8,9] Such persistence is usually associated with slowly varying external (boundary) forcing such as sea surface temperatures and anomaly patterns. On the scale of months to seasons, one of the most pronounced phenomenon is the El Nino Southern Oscillation (ENSO) event which occurs every 3–5 years and which strongly affects the weather over the tropical Pacific as well as over North America.[10] It has also been recently suggested that El Nino years are associated with increased rainfall over Eastern Mediterenean.[11] Although the link between extratropical weather/climate and sea surface temperature has been more difficult to establish, several recent studies have successfully proven that a connection exists on multiyear to decadal time scales between (i) the climate of North America and the North Pacific Ocean,[12] and (ii) the climate over Europe and the North Atlantic Ocean as expressed by the North Atlantic Oscillation (NAO) index.[8,9,13] On the even longer multidecadal to century time scales, external forcing associated with anthropogenic effects (e.g. increasing greenhouse gases and changing land use) also appear to play an important role in addition to the natural variability of the climate system.[14] Clearly separating the anthropogenic forcing from the natural variability of the atmosphere may prove to be a major challenge since the anthropogenic signal may project onto and therefore be hidden in the modes of natural climate variability.[15]

To avoid detection of spurious correlations arising from nonstationarities, new statistical-physics tools (wavelet techniques (WT) and detrended fluctuation analysis (DFA)) have been developed recently (see, e.g. Refs. 16–19). DFA and WT can systematically eliminate trends in the data and thus reveal intrinsic dynamical properties such as distributions, scaling and long-range correlations very often masked by nonstationarities. In a recent series of studies[20] we have used DFA and WT to study temperature correlations in different climatic zones on the globe. The results indicate that a universal long range power law correlation may exist which governs atmospheric variability at all spatiotemporal scales: The persistence, characterized by the auto-correlation $C(s)$ of temperature variations separated by s days, approximately decays as

$$C(s) \sim s^{-\gamma}, \tag{1}$$

with roughly the same exponent $\gamma \simeq 0.7$ for all stations considered. The range of this universal persistence law exceeds one decade, and is possibly even longer than the range of the temperature series considered. There are two major consequences:

- Conventional methods based on moving averages can no longer be used to separate trends from fluctuations.
- Conventional methods for the evaluation of the frequency of extreme low or extreme high temperatures are based on the hypotheris that the temperature fluctuations are essentially uncorrelated. The appearance of long range correlations sheds doubts on these methods.

1.2 The Modeling Approach

Regarding the modeling approach towards simulating and explaining atmospheric variability on various time scales, major progress has been made during the last two decades. Today, the research community routinely and extensively makes use of atmospheric, oceanic and coupled ocean-atmosphere circulation models where the major physical processes are included. Moreover, these models include representations of land-surface processes, sea-ice related processes and many other complex forcing mechanisms within the climate system. All processes are represented by mathematical equations which are solved numerically using a three-dimensional grid with a domain, resolution, and complexity determined by the topic of interest. For very long time integrations of thousands of years it is impossible to apply full general circulation models (GCM) due to their extremely high computational demand. Consequently, intermediate complexity models are used in these cases.

For global climate simulations on time scales ranging from months to decades or centuries, GCMs are used with typical resolutions of 200–300 km in the horizontal and 1 km in the vertical.[21] For regional climate simulations, similar models are used but the domain is limited to a few thousand km and the horizontal resolution is typically increased to 50 km or less.[22,23] In any case the grid resolution can never explicitly simulate all relevant scales of motion. This necessitates the parameterization of the smaller, subgrid scale processes such as cloud physics, radiative transfer, and macroscale turbulent mixing. Recently, it has also been found that previously neglected processes such as dust induced heating may also be important.[24]

The state-of-the-art coupled ocean-atmosphere general circulation models are able to simulate many of the important large-scale features of the climate system rather well. This includes seasonal, horizontal and vertical variations. They also explain the response to greenhouse gases and aerosols in terms of physical processes. In addition to this, other less pronounced variations in climate are reproduced with reasonable accuracy (e.g. the relationship between El Nino and rainfall in Central America and the northern part of South America).

The systematic evaluation and intercomparison of climate model results has proven to be a useful and effective mechanism for identifying common model weaknesses. In general, evaluations have been conducted for the atmospheric, oceanic, land-surface and sea-ice components of the models, and for the sensitivity of the links among these components. Until now these validations have not addressed the question of whether such models can reproduce the long-term climate memory in an appropriate way. If the simulations of the model are valid, then the patterns and relationships discovered by analyzing real observations and data must also be identifiable in the virtual world as represented by the model outputs.

This article is organized as follows: In Secs. 2 and 3 we describe the detrending methods and its application to temperature records of several meteorological stations around the

globe. In Sec. 4 we show how the current GCMs can be tested by applying the detrending techniques of Sec. 2 to the model data. We show that we can judge the models by their ability of reproducing the proper type of trends and long-range correlations inherent in the real data.

2. RECORD ANALYSIS

Consider, e.g. a record T_i of maximum daily temperatures measured at a certain meteorological station. The index i counts the days in the record, $i = 1, 2, \ldots, N$. For eliminating the periodic seasonal trends, we concentrate on the departures of the T_i, $\Delta T_i = T_i - \overline{T}_i$, from the mean maximum daily temperature $\overline{T}_i$ for each calendar date i, say 1st of April, which has been obtained by averaging over all years in the temperature series.

There exist two powerful detrending analysis methods: (a) the detrended fluctuation analysis (DFA) and (b) the wavelets methods (WT). The DFA was originally developed by Peng et al.[18] to investigate long-range correlations in DNA sequences and heart beat intervals, where nonstationarities similar to the nonstationarities in the temperature records[20] can occur. The wavelet methods in general are very convenient techniques to investigate fluctuating signals.[25] In this article we shall focus on the DFA. A very useful introduction to the wavelet technique with several applications is given in.[26]

Both DFA and wavelets techniques have been used to analyze the correlation function $C(s)$ of temperature records. The correlation function describes, how the persistence decays in time. $C(s)$ is defined by $C(s) = \langle \Delta T_i \Delta T_{i+s} \rangle$. The average $\langle \ldots \rangle$ is over all pairs with same time lag s. For reducing the level of noise present in the finite temperature series, we consider the "temperature profile"

$$Y_n = \sum_{i=1}^{n} \Delta T_i, \quad n = 1, 2 \ldots N\,. \tag{2}$$

We can consider the profile Y_n as the position of a random walker on a linear chain after n steps. The random walker starts at the origin and performs, in the ith step, a jump of length ΔT_i to the right, if ΔT_i is positive, and to the left, if ΔT_i is negative. According to random walk theory, the fluctuations $F^2(s)$ of the profile, in a given time window of size s, are related to the correlation function $C(s)$. For the relevant case (1) of long-range power-law correlations, $C(s) \sim s^{-\gamma}, 0 < \gamma < 1$, the mean-square fluctuations $\overline{F^2(s)}$, obtained by averaging over many time windows of size s (see below) increase by a power law,[27]

$$\overline{F^2(s)} \sim s^{2\alpha}, \quad \alpha = 1 - \gamma/2\,. \tag{3}$$

For uncorrelated data (as well as for correlations decaying faster than $1/s$), we have $\alpha = 1/2$.

To find how the square-fluctuations of the profile scale with s, we first divide each record of N elements into $K_s = [N/s]$ nonoverlapping subsequences of size s starting from the beginning and K_s nonoverlapping subsequences of size s starting from the end of the considered temperature series. We determine the square-fluctuations $F_\nu^2(s)$ in each segment ν and obtain $\overline{F^2(s)}$ by averaging over all segments. When plotted in a double logarithmic way, the fluctuation function

$$F(s) \equiv [\overline{F^2(s)}]^{\frac{1}{2}} \sim s^{\alpha} \tag{4}$$

is a straight line at large s values, with a slope $\alpha > \frac{1}{2}$ in the case of long range correlations.

The various methods differ in the way, the fluctuation function is calculated.

2.1 Fluctuation Analysis (FA)

In the simplest type of analysis (where trends are not going to be eliminated), we obtain the fluctuation functions just from the values of the profile at both endpoints of the νth segment,

$$F_\nu^2(s) = [Y_{\nu s} - Y_{(\nu-1)s}]^2, \tag{5}$$

and average $F_\nu^2(s)$ over the $2K_s$ subsequences

$$\overline{F^2(s)} = (1/K_s) \sum_{\nu=1}^{K_s} F_\nu^2(s)\,. \tag{6}$$

Here, $\overline{F^2(s)}$ can be viewed as mean square displacement of the random walker on the chain, after s steps. We obtain Ficks diffusion law $\overline{F^2(s)} \sim s$ for uncorrelated ΔT_i values.

We like to note that this fluctuation analysis corresponds to the R/S method introduced by Hurst (for a review, see e.g. Ref. 28). Since both methods do not eliminate trends, they do not give a clear picture when used alone. In many cases they can not distinguish between trends and long-range correlations when applied to a time records without supplementary calculations.

2.2 Detrending Fluctuation Analysis (DFA)

There are different orders of DFA that are distinguished by the way the trends in the data are eliminated. In lowest order (DFA1) we determine, for each subsequence ν, the best *linear* fit of the profile, and identify the fluctuations by the standard deviation $F_\nu^2(s)$ of the profile from this straight line. This way, we eliminate the influence of possible linear trends on scales larger than the segment sizes. Note that linear trends in the profile correspond to patch-like trends in the original record. DFA1 has been proposed originally by Peng et al.[18] when analyzing correlations in DNA.

DFA1 can be generalized straightforwardly to eliminate higher order trends: In second order DFA (DFA2) one calculates the standard deviations $F_\nu^2(s)$ of the profile from best *quadratic* fits of the profile, this way eliminating the influence of possible linear and parabolic trends on scales larger than the segment considered. In general, in the nth-order DFA technique, we calculate the deviations of the profile from the best nth-order polynomial fit and can eliminate this way the influence of possible $(n-1)$th-order trends on scales larger than the segment size.

It is essential in the DFA-analysis that the results of several orders of DFA (e.g. DFA1–DFA5) are compared with each other. The results are only reliable when above a certain order of DFA they yield the same type of behavior.[29] When compared with FA one can get additional insight into possible nonstationarities in the data.

3. ANALYSIS OF TEMPERATURE RECORDS

Figures 1 and 2 show the results of the FA and DFA analysis of the maximum daily temperatures T_i of the following weather stations (the length of the records is written within the parentheses): Luling (USA, 90 y), and Kasan (Russia, 96 y) [Figs. 1(a) and (c)], Tuscon (USA, 97 y), Melbourne (136 y), Seoul (86 y), Prague (218 y) Figs. 2(a)–(d)]. The results are typical for a large number of records that we have analyzed so far (see Ref. 20).

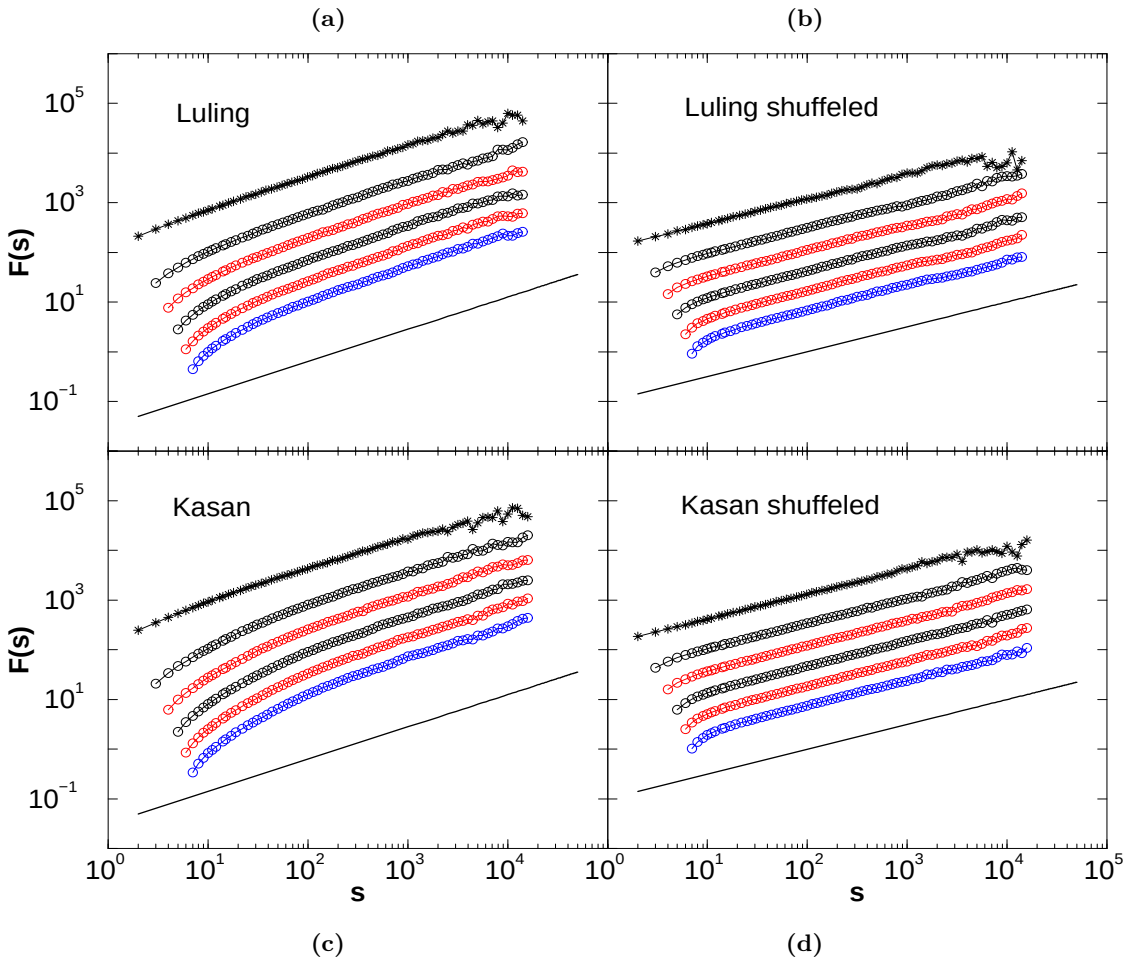

Fig. 1 Analysis of daily maximum temperature records of Luling and Kasan. The analysis of the real data shown in **(a)** and **(c)** is compared with the analysis of the corresponding shuffled data shown in **(b)** and **(d)**. The four figures show the fluctuation functions obtained by FA, DFA1, DFA2, DFA3, DFA4, and DFA5 (from top to bottom) for the four sets of data. The scale of the fluctuation functions is arbitrary.

In the log-log plots, all curves are (except at small s-values) approximately straight lines, with a slope $\alpha \cong 0.65$. There exists a natural crossover (above the DFA-crossover) that can be best estimated from FA and DFA1. As can be verified easily, the crossover occurs roughly at $t_c = 10d$, which is the order of magnitude for a typical Grosswetterlage. Above t_c, there exists long-range persistence expressed by the power-law decay of the correlation function with an exponent $\gamma = 2 - 2\alpha \cong 0.7$. The results seem to indicate that the exponent is universal, i.e. does not depend on the location and the climatic zone of the weather station. Below t_c, the fluctuation functions do not show universal behavior and reflect the different climatic zones.

To test our claim that the slope $\alpha \cong 0.65$ is due to long-range correlations, and does not result from a singular behavior of the probalitity distribution function of the ΔT_i we have eliminated the correlations by randomly shuffling the ΔT_i. By definition this shuffling has no effect on the probability distribution function of the ΔT_i, which we found to be approximately Gaussian at large temperature variations. The right hand side of Fig. 1 [Figs. 1(b) and (d)] show the effect of shuffling on the fluctuation functions. By comparing the left hand sides of the figures with the right hand sides we see the effect of correlations.

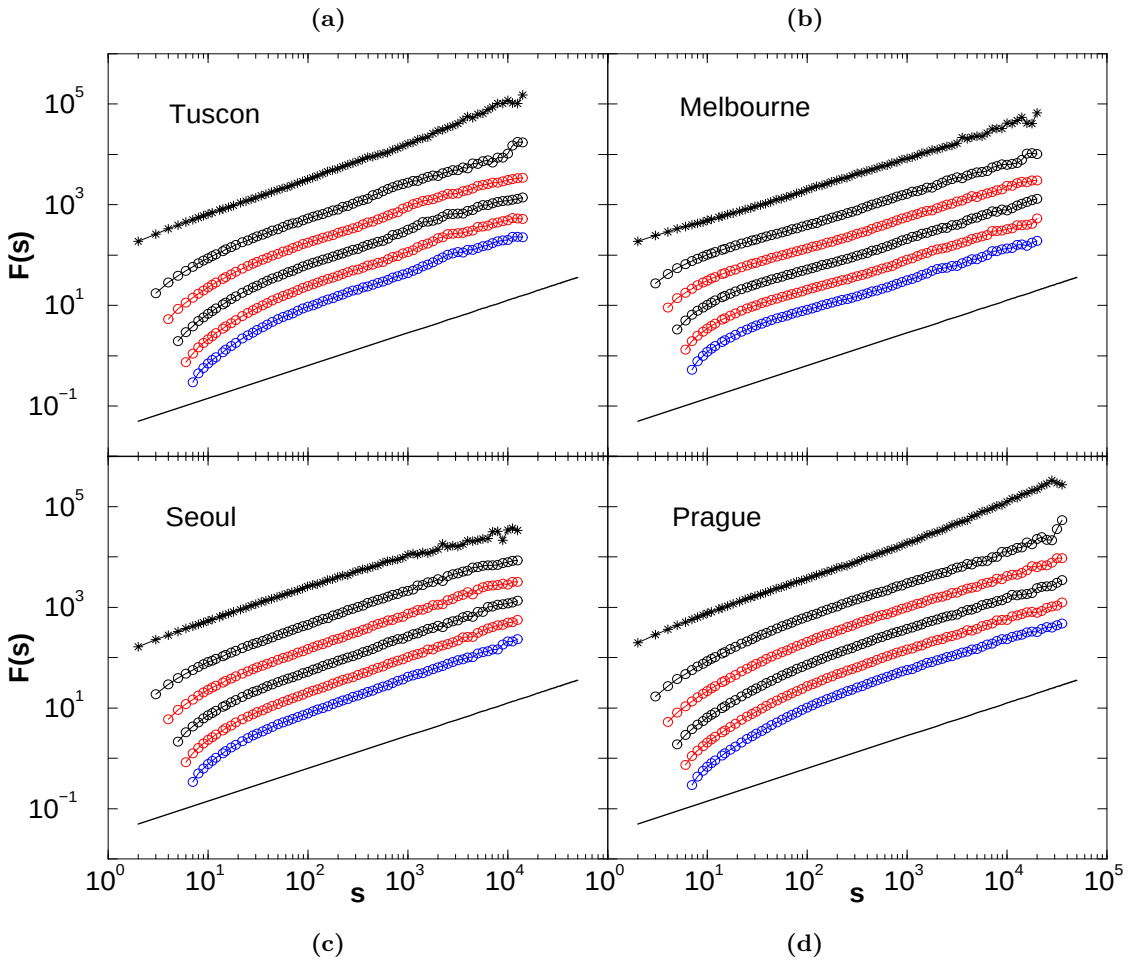

Fig. 2 Analysis of the daily maximum temperature records of Tucson, Melbourne, Seoul and Prague (as Fig. 1).

The exponent α characterizing the fluctuations in the shuffled uncorrelated sequence is 1/2, as expected.

Since the exponent does not depend on the location of the meteorological station and its local environment, the power law behavior can serve as an ideal test for climate models where regional details cannot be incorporated and therefore regional phenomena like urban warming cannot be accounted for. The power law behavior seems to be a global phenomenon and therefore should also show up in the simulated data of the GMCS. As mentioned earlier, the presence of long range correlations has far-reaching consequences on the possible detection of trends directly from the record and on the evaluation of extreme events.

4. ANALYSIS OF SIMULATED TEMPERATURE RECORDS

Next we turn to the analysis of simulated data that were obtained by four general circulation models around Praque. We have chosen Prague, since the Prague record is the longest record we could get. The models are:

- 1. GFDL-R15-a

  This is the latest version of a coupled atmosphere-ocean model (AOGCM) that has been developed over many years.[30,31] The atmosperic sub-model is a spectral model with a

horizontal truncation of rhomboidal 15 (R15), a transform grid of 48×40 longitude-latitude points (7.5×4.5 degrees), and nine vertical levels. The ocean sub-model is a grid point model with a latitude-longitude grid spacing of 4.5×3.75 degrees and 12 vertical layers. To reduce model drift, flux corrections are applied to the heat and water fluxes at the surface. In the control run, the CO_2 concentration is kept fixed at the 1958 value while for the climate change greenhouse gases are represented by equivalent CO_2 concentrations which increase at a rate of roughly 1% per year according to the IPCC IS92a scenario.[32]

- 2. CSIRO-Mk2
  The CSIRO model is a coupled AOGCM which contains atmospheric, oceanic, sea-ice and biospheric sub-models. The atmospheric sub-model is a spectral model with R21 truncation, a transform grid of 64×56 longitude-latitude points (5.6×3.2 degrees), and nine vertical layers. The ocean sub-model is a grid point model that uses the same horizontal grid as the atmosphere and has 21 vertical levels. Flux correction at is applied to the heat, fresh water, and momentum fluxes at the surface. All greenhouse gases are combined into an equivalent CO_2 concentration which follows observations from 1880 to 1989 and are then pojected into the future according to the IS92a scenario.[32] This model was developed during the years 1994–1995.[33,34]

- 3. ECHAM4/OPYC3
  The coupled AOGCM ECHAM4/OPYC3 was developed as a cooperative effort between the Max-Planck-Institut für Meteorologie (MPI) and Deutsches Klimarechenzentrum (DKRZ) in Hamburg. The atmospheric model was derived from the European Centre for Medium Range Weather Forecasts (ECMWF) model. It is a spectral model with triangular truncation T42, a longitude-latidue transform grid of 128×64 points (2.8 degrees), and 19 vertical levels. The ocean model (OPYC3) is a grid point model with 11 isopycnal layers and it is run on the same grid as the atmosphere. Flux correction is applied to the heat, fresh water and momentum fluxes at the surface.[35–37] Historic greenhouse gas concentrations are used from 1860–1989 and from 1990 onward they are projected according to the IS92a scenario.

- 4. HADCM3
  HADCM3 is the latest version of the coupled AOGCM developed at the Hadley Centre.[38] Unlike the other models described above, here the atmospheric model is a grid point model with a longitude-latitude grid of 96×73 points (3.75×2.5 degree spacing) and it has 19 vertical levels. The ocean model has a horizontal resolution of 1.25 degrees in both latitude and longitude and 20 vertical levels. No flux correction is applied at the surface. Historic greenhouse gas concentrations are used during the period 1860–1989. From 1990 and onward they are increased according to the IS95a scenario (a slightly modified version of IS92a).

For each model, we obtained the temperature records (mean monthly data) of the four grid points closest to Prague from the internet.[39] We interpolated the data at the location of Prague.

Figure 3(a) shows the results of the FA- and DFA-Analysis for the real temperature record of Prague that starts in 1775 and ends in 1992. Figures 3(b)–(d) show the results obtained from ECHAM4, CSIRO and HADCM, that end up at the same year as the real record. The available data of GFDL cover only 40y, so we do not present them here.

We are interested in the way the models can reproduce the actual data regarding (a) trends and (b) long-range correlations. Of course, we cannot expect the models to reproduce local

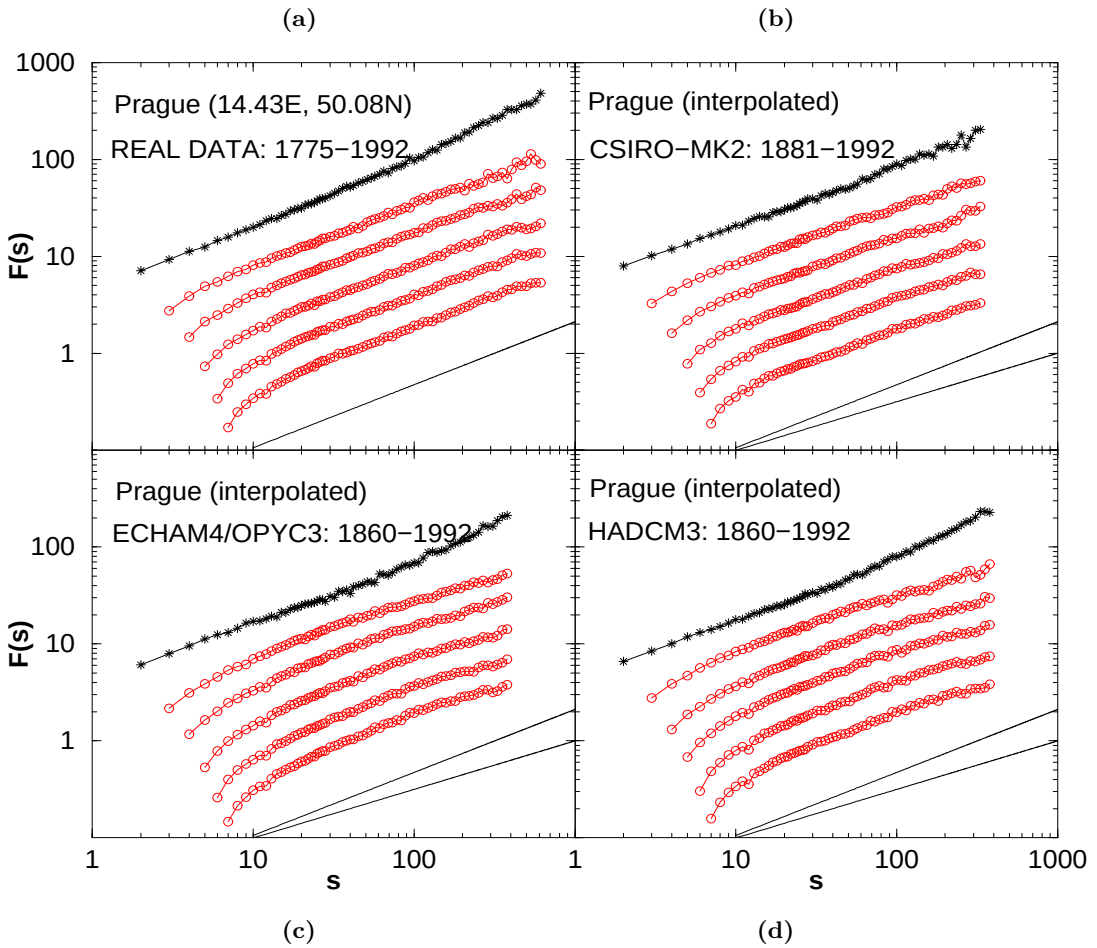

Fig. 3 FA- and DFA-Analysis of **(a)** the monthly mean temperature record of Prague and **(b)** simulated interpolated monthly mean temperature records at the geographical position of Prague, for three general circulation models: **(b)** CSIRO, **(c)** ECHAM4 and **(d)** HADCM3. The four figures show the fluctuations functions obtained by FA, DFA1, DFA2, DFA3, DFA4 and DFA5 (from top to bottom) for the four sets of data. The scale of the fluctuations is arbitrary (after Govindan et al.).[40]

trends like urban warming or short-term correlation structures. But the long-range correlations we discussed in the previous section show characteristic universal features that are actually independent of the local environment around a station. So we can expect that successful models with good prognostic features will be able to reproduce them.

As discussed already above (for the daily data), the FA- and DFA fluctuation functions for the real temperature record of Prague have approximately the same slope of $\alpha \simeq 0.65$ in the double-logarithmic plot (shown as straight line in the figure). At large time scales there is a slight increase of the FA-function (which clearly indicates a weak trend). In contrast, the FA-results for the HADLEY and ECHAM4 data show a pronounced trend above 100 months represented by a large slope. For CSIRO, the FA-result is not so conclusive since they scatter considerably at large scales. It seems that two of the three models overestimate the trend in the past. Regarding scaling, the DFA curves for CSIRO show good straight lines in a double logarithmic presentation. The exponents are close to the exponents from the Prague record. In contrast, ECHAM4 and HADLEY show a crossover to an exponent $\alpha = 0.5$ after about 3 years. The exponent $\alpha = 0.5$ indicates loss of persistence. Hence ECHAM4 and HADLEY reproduce data sets that show a linear trend at large time scales and simultaneously the lack of correlations exceeding 3y, in contrast to the reality.

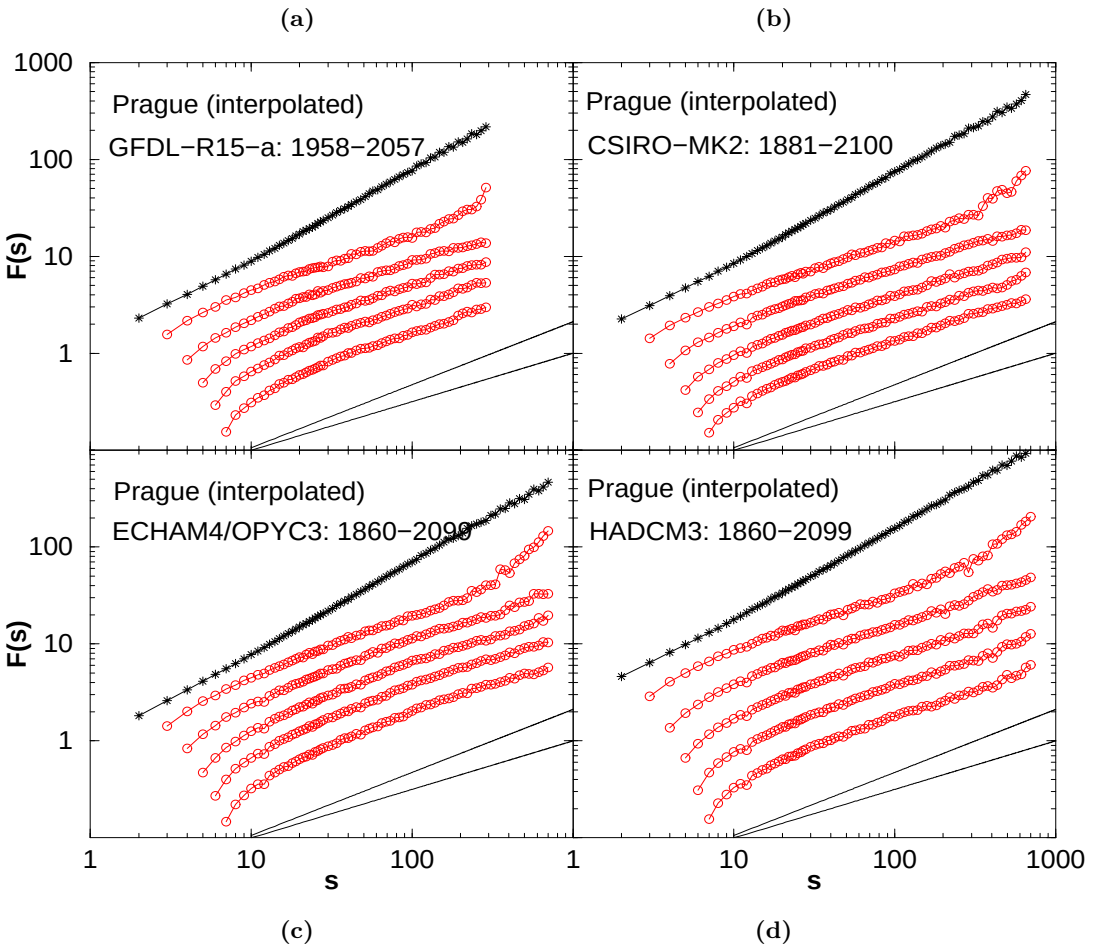

Fig. 4 FA- and DFA-Analysis of the simulated interpolated monthly mean temperature records of the geographical position of Prague, for four general circulation models: **(a)** GFDL, **(b)** CSIRO, **(c)** ECHAM4 and **(d)** HADCM3. While Fig. 3 considered only data in the past, Fig. 4 considers the whole set of data (past and future). The data is available in the internet[39] and, the analysis is after Govindan et al.[40]

The scaling features remain very similar when the data sets from the models are extended into the 21st century (see Fig. 4).[40] We consider this an important issue, since it shows an internal consistency of the models. However, the trends, which show up in FA and DFA1, are much more pronounced compared to the data from Fig. 3.

We have obtained similar qualitative behavior also for other simulated temperature record. From the trends, one estimates the warming of the atmosphere in the future. Since the trends are almost not visible in the real data and overestimated by the models in the past, it seems possible that the trends are also overestimated by the models in the future. From this point of view it cannot be excluded that the global warming in the next 100y will be less pronounced than predicted by the models.

REFERENCES

1. IPCC, *The Regional Impacts of Climate Change. An Assessment of Vulnerability* (University Press, Cambridge, 1998).
2. P. M. Blaikie, T. Cannon, I. Davi and B. Wisner, *At Risk*: *Natural Hazards, Vulnerability and Disasters* (Routledge, London, 1994).
3. H. Grassl, "Global Climate Change," *Interdisc. Sci. Rev.* **24**(3), 185–194 (1999).

4. H. J. Schellnhuber, *Nature* **402**(6761), C19–C23 Suppl. (1999).
5. K. Hasselmann, *Clim. Dynam.* **13**, 601 (1997), and the references therein.
6. J. G. Charney and J. G. Devore, *J. Atmos. Sci.* **36**, 1205 (1979).
7. J. Shukla, *Science* **282**, 728–731 (1998).
8. R. L. Molinari, D. A. Mayer, J. F. Festa and H. F. Bezdek, *J. Geophys. Res.* **102**, 3267 (1997).
9. R. T. Sutton and M. R. Allen, *Nature* **388**, 563 (1997).
10. S. G. Philander, *El Nino, La Nina and the Southern Oscillation.* International Geophysics Series, Vol. 46, 1990.
11. C. Price, L. Stone, A. Huppert, B. Rajagopalan and P. Alpert, *Geophys. Res. Lett.* **25**, 3963 (1998).
12. M. Latif and T. P. Barnett, *Science* **266**, 634–637 (1994).
13. M. J. Rodwell, D. P. Rodwell and C. K. Folland, *Nature* **398**, 320–323 (1999).
14. K. Hasselmann, *Science* **276**, 914–915 (1997).
15. S. Corti, F. Molteni and T. N. Palmer, *Nature* **398**, 799–802 (1999).
16. P. Ch. Ivanov, A. Bunde, L. A. N. Amaral, S. Havlin, J. Fritsch-Yelle, R. M. Baevsky, H. E. Stanley and A. L. Goldberger, *Europhys. Lett.* **48**(59), 4 (1999).
17. A. Bunde, S. Havlin, J. W. Kantelhardt, T. Penzel, J. H. Peter and K. Voigt, *Phys. Rev. Lett.* **85**, 3736 (2000).
18. C.-K. Peng, S. V. Buldyrev, A. L. Goldberger, S. Havlin, F. Sciortino, M. Simons and H. E. Stanley, *Nature* **356**, 168 (1992); S. V. Buldyrev, A. L. Goldberger, S. Havlin, C. K. Peng, M. Simons and F. Sciortino, *Phys. Rev. Lett.* **71**, 1776 (1993); S. V. Buldyrev, A. L. Goldberger, S. Havlin, R. N. Mantegna, M. E. Matsa, C.-K. Peng, M. Simons and H. E. Stanley, *Phys. Rev.* **E51**, 5084 (1995).
19. A. Arneodo, E. Bacry, P. V. Graves and J. F. Muzy, *Phys. Rev. Lett.* **74**, 3293 (1995); A. Arneodo et al., *Physica* **D96**, 291 (1996).
20. E. Koscielny-Bunde, A. Bunde, S. Havlin, H. E. Roman, Y. Goldreich and H.-J. Schellnhuber, *Phys. Rev. Lett.* **81**, 729 (1998); E. Koscielny-Bunde, H. E. Roman, A. Bunde, S. Havlin and H. J. Schellnhuber, *Phil. Mag.* **B77**, 1331 (1998); E. Koscielny-Bunde, A. Bunde, S. Havlin and Y. Goldreich, *Physica* **A231**, 393 (1996).
21. R. Voss and U. Mikolajewicz, Max-Planck-Institut fur Meteorologie, Report No. 298 (1999); S. Brenner, *J. Climate* **9**, 3337 (1996).
22. F. Giorgi, *J. Climate* **3**, 941–963 (1990).
23. E. S. Takle, W. J. Gutowski Jr., R. W. Arritt, Z. Pan, C. Anderson, R. Silva, D. Caya, S. Chen, J. H. Christensen, S-Y. Hong, H.-M. H. Juang, H. Katzfey, W. Lapenta, R. Laprise, P. Lopez, J. McGregor and J. R. Roads, "Project to Intercompare Regional Climate Simulations (PIRCS)," *J. Geophys. Res.*, in press (1999).
24. P. Alpert, Y. J. Kaufman and Y. Shay-El, *Nature* **395**(6700), 367–370 (1998).
25. M. Vetterli and J. Kovacevic, *Wavelets and Subbane Coding* (Prentice Hall, Englewood Cliffs, New Jersey, 1995).
26. A. Arneodo, E. Bacry, P. V. Graves and J. F. Muzy, in *The Science of Disasters*, eds. A. Bunde, J. Kropp and H. J. Schellnhuber (Springer, Berlin, 2001).
27. A. Bunde and S. Havlin (eds.), *Fractals in Science* (Springer, New York, 1995).
28. J. Feder, *Fractals* (Plenum, New York, 1989).
29. J. W. Kantelhardt, E. Koscielny-Bunde, H. A. Rego, A. Bunde and S. Havlin, *Physica A*, in press (2001).
30. S. Manabe, R. J. Stouffer, M. J. Spelman and K. Bryan, *J. Climate* **4**, 785 (1991).
31. S. Manabe, M. J. Spelman and R. J. Stouffer, *J. Climate* **5**, 105 (1992).
32. J. Leggett, W. J. Pepper and R. J. Swart, in *Climate Change 1992: The Supplementary Report to the IPCC Scientific Assessment*, eds. J. T. Houghton, B. A. Callander and S. K. Varney (Cambridge University Press, Cambridge, 1992).
33. H. B. Gordon and S. P. O'Farrell, *Mon. Wea. Rev.* **125**, 875 (1997).
34. A. C. Hirst, H. B. Gordon and S. P. O'Farrell, *Geophys. Res. Lett.* **23**, 3361 (1996).
35. L. Bengtsson, K. Arpe and E. Roeckner et al., *Clim. Dynam.* **12**(4), 261 (1996).
36. ECHAM3, *Atmospheric General Circulation Model*, ed. Dkrz-Model User Support Group (October 1996).

37. *The OPYC Ocean General Circulation Model*, ed. Joseph M. Oberhuber (October 1992). Deutsches Klimarechenzentrum (DKRZ), Report No. 7, (1997).
38. C. Gordon, C. Cooper and C.A. Senior et al., *Clim. Dynam.* **16**(2–3), 147 (2000).
39. Internet address: http://*ipcc* − *ddc.cru.uca.ac.uk/dkrz/dkrz* − *index.html*
40. Govindan et al., *Physica A*, in press.